$L_{2,3}$ x-ray-absorption edges of d^0 compounds: K^+, Ca^{2+}, Sc^{3+}, and Ti^{4+} in O_h (octahedral) symmetry

F. M. F. de Groot and J. C. Fuggle
Research Institute for Materials, University of Nijmegen, Toernooiveld, 6525 ED Nijmegen, The Netherlands

B. T. Thole and G. A. Sawatzky
Materials Science Centre, University of Groningen, Nijenborgh 18, Paddepoel, 9747 AG Groningen, The Netherlands

(Received 17 July 1989)

The $L_{2,3}$ x-ray-absorption edges of $3d^0$ compounds are calculated with use of an atomic description of the $2p^6 3d^0$ to $2p^5 3d^1$ excitation, with the inclusion of the crystal field. For reasons of clarity, we confine ourselves to d^0 compounds in octahedral symmetry, but the same approach is applicable to all other d^N compounds in any point-group symmetry. The experimental spectra of $FeTiO_3$, Sc_2O_3, ScF_3, CaF_2, and the potassium halides are well reproduced by the present calculations, including the previously misinterpreted small leading peaks. The splitting between the two main peaks in both the L_3 and L_2 edge are related, though not equal, to the crystal-field splitting. Comparison to experiment showed that the broadening of the main multiplet lines is different. This can be related to Coster-Kronig Auger processes for the L_2 edge and to a solid-state broadening which is a combination of vibrational (phononic) and dispersional broadenings. With the full treatment of the atomic multiplets, the atomic effects can be separated from solid-state effects, which offers a better description of the latter. This includes vibrational broadenings, the covalent screening of the intra-atomic Coulomb and exchange interactions, via the position of small leading peaks, and surface effects. The same general framework can be used to discuss crystal-field effects in both lower symmetries, with the possibility of polarization-dependent spectra (e.g., TiO_2), and partly filled d bands.

I. INTRODUCTION

In the past few years experimental progress in the field of soft-x-ray absorption has been tremendous. The attainable experimental resolution has improved to its present best value of 30 meV at 300 eV.[1,2] This technical progress has opened the possibility to measure the transition metal $L_{2,3}$ x-ray-absorption edges, including also K and Ca, with great accuracy.[3]

Theoretical developments have lagged behind those of experiment but the improvement in resolution has created the need for a much more advanced description. In this paper we contribute to a description of the transition metal $L_{2,3}$ x-ray-absorption spectra.[4] The starting point is an atomic multiplet calculation.[5–7] We then treat those cases where the most prominent effect of the solid state is the crystal field, the breaking of the spherical symmetry around the atom. We prefer to use the term crystal field rather than ligand field, because in principle we only change the point-group symmetry. The crystal field is put in as a parameter fit to the experiment. In this manner the hybridization effect of the ligands is implicitly taken into account. Dispersional effects, which have been treated earlier for the elemental transition metals,[8,9] are not taken explicitly into account here.

Using group-theory formalism,[10–12] it is possible to project the atomic spectrum (spherical symmetry) onto a specific symmetry group. All point-group symmetries can be addressed in this way. However, the lower the symmetry, the more parameters are needed to account for all possible interactions. In this paper we only consider O_h symmetry, which accounts for both sixfold (octahedral) and eightfold (simple-cubic) surroundings. We will show that with the restriction to O_h symmetry we are already able to obtain excellent results, even for some cases in which the actual symmetry is lower. To limit the complexity of the theory presented, we postpone the discussion of lower symmetries.

We start with an outline of the theoretical approach (Sec. II). In Sec. III we will present some general results for the d^0 compounds, where we take Ti^{4+} as an example. We show that the splittings in the x-ray-absorption spectroscopy (XAS) spectrum are due to, but do not directly scale with, the crystal-field parameter $10Dq$. In Sec. IV we will make a comparison to experimental results of K^+, Ca^{2+}, Sc^{3+}, and Ti^{4+} compounds.

II. THEORY

We calculated the excitation from the d^0 ground state to the final-state $2p^5 3d^1$ multiplet by means of an optical dipole transition. The central point in our analysis will be the crystal field. First it is necessary, however, to calculate the atomic multiplet.

A. Atomic multiplet theory

For reasons of clarity we will briefly repeat atomic multiplet theory as can be found in the standard text-

books.[13,14] The Hamiltonian for atomic multiplets can be written as

$$H = H_{\text{av}} + \mathbf{L}\cdot\mathbf{S}(p) + \mathbf{L}\cdot\mathbf{S}(d) + g(i,j) .$$

H_{av} consists of the kinetic term and the interaction with the nuclei. It gives the average energy of the multiplet and does not contribute to the multiplet splittings. The splittings in the multiplet are caused by the spin-orbit couplings, $\mathbf{L}\cdot\mathbf{S}$, for the $2p$ and $3d$ electron, and by the Coulomb repulsion term, $g(i,j)$. This two-electron operator can be expressed in terms of spherical harmonics,[13] which necessitates the division of radial and angular parts. The radial part, $R^K(l_1 l_2; l_3 l_4)$ is divided in direct Coulomb terms, $F^K(l_1 l_2; l_1 l_2)$, and exchange terms, $G^K(l_1 l_2; l_2 l_1)$. The angular part of $g(i,j)$ results in the selection rules, or in other words it gives the possible K values. For the direct Coulomb term, no odd K values are allowed, and the maximum K value is two times the minimal l value. For the p^5d^1 multiplet this results in F^0 and F^2, while for a d^2 multiplet F^4 also comes into play. The K values in the exchange term equal $|l_1 - l_2|$, $|l_1 - l_2 + 2k|, \ldots, l_1 + l_2$. For the p^5d^1 multiplet this results in G^1 and G^3. Thus we can evaluate the two-electron operator $g(i,j)$ for the p^5d^1 multiplet in terms of four interactions: F^0, F^2, G^1, and G^3. F^0 only contributes to the average energy and is taken into H_{av}. The *ab initio* calculated Coulomb, exchange and spin-orbit parameters (F^2, G^1, G^3, $\mathbf{L}\cdot\mathbf{S}_p$, and $\mathbf{L}\cdot\mathbf{S}_d$) of K^+, Ca^{2+}, Sc^{3+}, and Ti^{4+} are given in Table I. For the actual crystal-field calculations, the *ab initio* (Hartree-Fock) values of F^2, G^1, and G^3 are scaled down to 80% of their original value to account for many-body corrections.[15]

B. The atomic excitation from $2p^63d^0$ to $2p^53d^1$

The ground state d^0 consists of one single ^1S state. Therefore with x-ray absorption, following the optical transition selection rule, only the ^1P final state is within reach in LS coupling, thus only one peak would appear in the XAS spectrum. Turning on the spin-orbit coupling of the $2p$ core hole, but still neglecting the spin-orbit coupling of the $3d$ electron and the Coulomb repulsion term, $g(i,j)$, leads to the well-known approximation of two peaks with an intensity ratio of 1:2, denoted by the L_3 and L_2 edge. This is caused by the transformation from LS to jj coupling which results in the mapping of ^1P (LS) onto ^1P, ^3P, and ^3D (jj), of which both triplet states have equal energy.[8] As is directly evident from the values of Table I, the direct Coulomb and exchange terms F^2, G^1, and G^3 are not negligible. The result is a splitting of the L_3 edge and consequently three absorption lines. The intensities of these lines are also strongly redistributed by F^2, G^1, and G^3. Figure 1 gives only the result for Ti^{4+} as the atomic spectra for K^+, Ca^{2+}, and Sc^{3+} are similar. The small leading peak has predominantly triplet character and is mixed through the spin-orbit interaction and the Coulomb repulsion into the main L_3 edge. This small leading peak retains its intensity when the crystal field is considered and will give rise to a general small leading peak in x-ray-absorption spectra of d^0 compounds. We stress this atomic multiplet feature as it has been overlooked in some x-ray-absorption literature.

C. Crystal-field effect on the $2p^53d^1$ multiplet

We now consider the crystal field. In terms of group theory the effect of an octahedral crystal field is the reduction of symmetry from O_3 to O_h. All irreducible representations (henceforth referred to as IR) in spherical symmetry are projected onto the O_h group. We have to consider separately (1) the ground state IR, (2) the final state IR's, and (3) the transition IR.

Using jj coupling in O_3 symmetry, there exists one IR per J value, with a degeneracy of $2J+1$. The d^0 ground state has a J value of 0, and the transition has a J value of 1. The accessible final states are thus restricted to those with a J value of 1. The 60 possible states of the p^5d^1 multiplet are distributed over five IR's with J values of 0, 1, 2, 3, and 4, and with degeneracies of, respectively, 1, 3, 4, 3, and 1. Notice that in LS coupling the p^5d^1 multiplet has six IR's: singlet and triplet F, D, and P.

We have to transform these O_3 IR's to O_h symmetry, where there are five possible IR's. Their standard notation is A_1, A_2 (one-dimensional), E (two-dimensional), T_1, and T_2 (Ref. 14) (three-dimensional). The transformation from O_3 to its subgroup O_h, mostly called the O_3-O_h branching, can be found in the work of Butler.[10]

TABLE I. Values for the atomic multiplet, from an *ab initio* calculation. E_{av} gives the average energy of the multiplet and $\mathbf{L}\cdot\mathbf{S}$ gives the parameters for the spin-orbit coupling. The *ab initio* value of the Coulomb and exchange parameters or Slater integrals F^2, G^1, and G^3 are given; they are normalized to 80% of their *ab initio* value in the real calculation, to simulate configuration interaction.

Ion	K^+	Ca^{2+}	Sc^{3+}	Ti^{4+}
E_{av}	298.40	350.37	405.75	464.81
$\mathbf{L}\cdot\mathbf{S}(p)$	1.88	2.4	3.03	3.78
$\mathbf{L}\cdot\mathbf{S}(d)$	0.005	0.011	0.020	0.032
F^2_{pd}	2.20	3.79	5.09	6.30
G^1_{pd}	1.32	2.51	3.58	4.62
G^3_{pd}	0.74	1.42	2.03	2.63

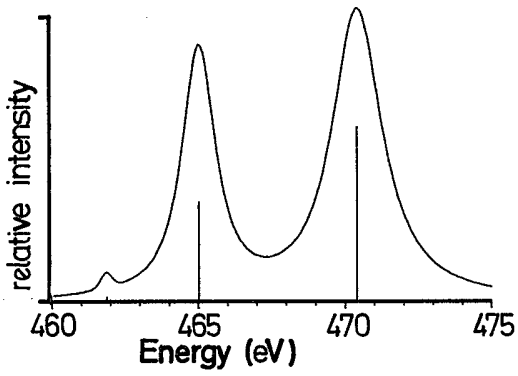

FIG. 1. Atomic multiplet spectrum for the $3d^0$ to $2p^53d^1$ excitation of Ti^{4+}; the Slater integrals are reduced to 80% of their Hartree-Fock values.

TABLE II. The branching table from O_3 to O_h is given for integer values of J in O_3 (as occur for the p^5d^1 multiplet). See Butler for more details and all other branching tables.

O_3	→	O_h
$J=0$	→	A_1
$J=1$	→	T_1
$J=2$	→	$E+T_2$
$J=3$	→	$T_1+T_2+A_2$
$J=4$	→	$A_1+T_1+E+T_2$

The essential details are repeated in Table II.

The ground state and the transition IR are transformed to, respectively, A_1 and T_1. The entire effect of the crystal field to split and shift the peaks in the spectrum is thus concentrated in the final state. All possible final states must have T_1 symmetry, otherwise the transition matrix element equals zero. The T_1 IR can be reached not only from the $J=1$ IR, but also from the $J=3$ and $J=4$ IR's (see Table II). The $J=1$ and $J=3$ IR's are both threefold degenerate and the $J=4$ IR is nondegenerate. This results in seven possible T_1 IR's in O_h symmetry, or, in other words, seven possible final states. The XAS spectrum consists, in principle, of seven lines, as can be seen in Fig. 2, where the Ti^{4+} XAS spectrum for a crystal-field splitting ($10Dq$) of 1.8 eV is calculated.

D. Generality of the method

The method used starts with the calculation of the atomic (initial and final) multiplets. The Slater integrals (F^2, G^1, and G^3) are scaled down to 80% of their *ab initio* values. Then the reduced matrix elements of all necessary operators in the spherical group are calculated with the use of Cowan's atomic multiplet program.[7] To obtain the reduced matrix elements in any point group, Butler's program is used for the calculation of all necessary factors ($3J$ symbols). With this general approach, the program is, in principle, capable of calculating the transition probabilities between any two configurations in XAS, x-ray photoemission spectroscopy (XPS), or bremsstrahlung isochromat spectroscopy (BIS) in all point-group symmetries.[7,16]

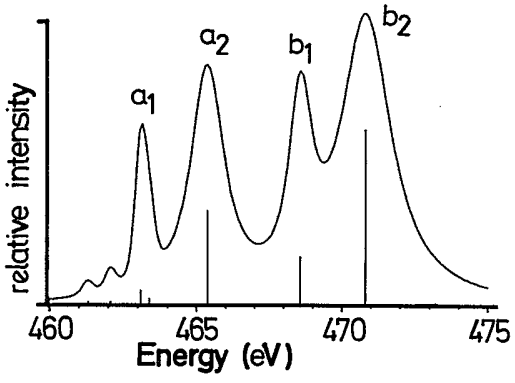

FIG. 2. Multiplet spectrum for the $3d^0$ to $2p^53d^1$ excitation of Ti^{4+} in octahedral symmetry; the crystal-field parameter $10Dq$ was taken as 1.8 eV. The 80% reduction of the Hartree-Fock values was used.

This means that for the $L_{2,3}$ XAS edges any transition from a d^N ground state to a p^5d^{N+1} final state can be calculated. The number of final states increases drastically if $N>0$. Also, ground-state crystal-field effects become important, which complicates the analysis. We have calculated the complete d^N series in O_h symmetry, which will be published elsewhere.[17] The calculation of lower symmetries, using the necessary branchings, means that the number of parameters increases. For example, O_h needs only one parameter while D_{4h} needs three, which makes the analysis more difficult. Another important effect of lower symmetries such as D_{4h} is the polarization dependence of the spectrum. The possibility to use lower symmetries to correctly describe x-ray-absorption spectra was used for rutile TiO_2.[18]

III. RESULTS FOR d^0 COMPOUNDS

Experimentally it is found that the crystal field splits the L_3 and L_2 x-ray-absorption edges. Often this is pictured as a splitting of both edges into two, with the energy difference between both peaks assumed equal to the crystal-field parameter $10Dq$. Using the crystal-field program we have calculated the p^5d^1 multiplet for a number of $10Dq$ values. Figure 3 gives the results for Ti^{4+} using both positive and negative values, related to, respectively, sixfold (octahedral) and eightfold (simple-cubic) surroundings. The crystal field has to compete with all intra-atomic interactions [F^2, G^1, G^3, $\mathbf{L}\cdot\mathbf{S}(p)$, and $\mathbf{L}\cdot\mathbf{S}(d)$]. The result is a complex change of the spectrum as a function of $10Dq$. The value of the crystal-field splitting is indicated as the distance between the vertical line and the diagonal. In Fig. 4 the distance between the two main peaks in the L_3 (peak a_1 and a_2) and L_2 (peak b_1 and b_2) edge is given as a function of the crystal field. The result is evident: *The energy splitting in the XAS spectra, is, in general, not equal to 10Dq.*

Starting with the atomic calculation (Fig. 4, $10Dq=0$) and turning on a small crystal field, a small energy splitting immediately appears. This does not mean that the atomic lines are split in two, but that other final states are mixed in. These states were not accessible in spherical symmetry as discussed in Sec. II. The intensities of these new transitions (opened channels for O_h) are small for low crystal fields as can be seen in Fig. 5.

The following picture then emerges: In O_h symmetry the p^5d^1 multiplet consists of seven lines, four of which are forbidden in spherical symmetry. The crystal field has the effect of (1) shifting the seven final states in energy (see Figs. 3 and 6) and (2) redistributing the absorption intensity over all seven lines (see Fig. 5).

The crystal field has a slightly different, though equivalent, effect on the L_3 edge, compared to the L_2 edge. This small difference between the L_3 and L_2 edge can also be seen in the experimental spectra, but this was not extensively discussed until now. With the present improvement in resolution,[2] it is possible to show the ine-

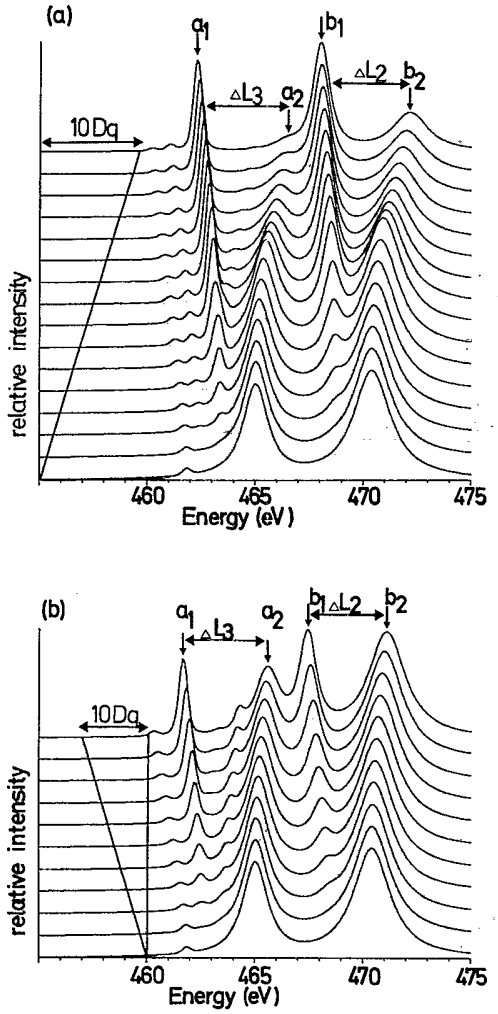

FIG. 3. Ti^{4+} $2p^5 3d^1$ excitation spectra in O_h symmetry as a function of the crystal-field splitting $10Dq$. (a) The value of $10Dq$ is positive and ranges from 0.0 to 4.5 eV, indicated by the diagonal line; (b) the value of $10Dq$ is negative. ΔL_3 measures the distance between the peaks a_1 and a_2, split by the crystal field.

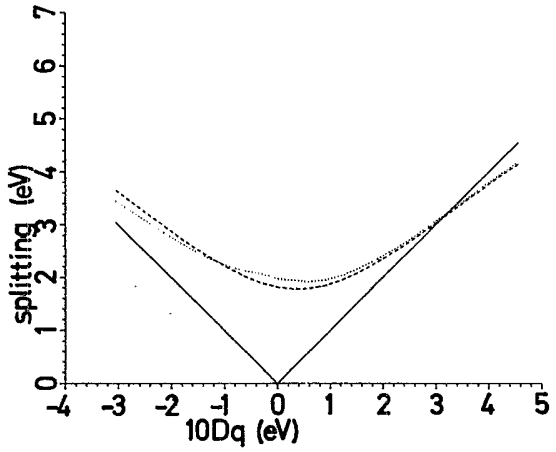

FIG. 4. The splitting between peaks a_1 and a_2 (ΔL_3, dashed line) and between peaks b_1 and b_2 (ΔL_2, dotted line) is given as a function of the crystal-field parameter $10Dq$. For the solid line, the assumption of a splitting equal to $10Dq$ is made.

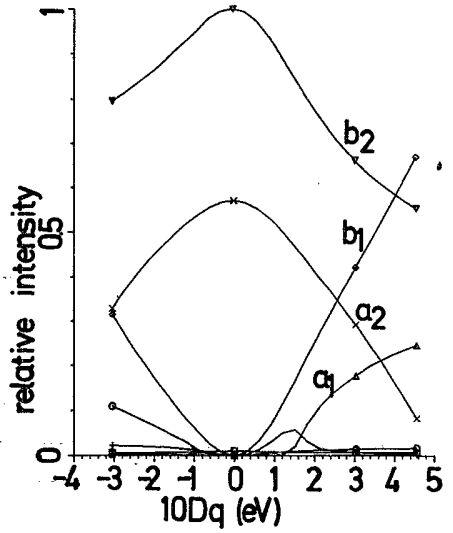

FIG. 5. For Ti^{4+} in O_h symmetry the changes in intensity are given as a function of the crystal-field splitting $10Dq$. The symbols correspond to the seven absorption lines ordered for increasing energy (see Fig. 6).

quivalence of peak separations in the L_2 and L_3 peaks convincingly. The clearest case is CaF_2 (see Sec. IV C).

IV. COMPARISON WITH EXPERIMENT

We compare our results for the $2p^5 3d^1$ optical transition multiplet with x-ray-absorption spectra for K^+, Ca^{2+}, Sc^{3+}, and Ti^{4+} compounds. We start with Ti^{4+} in ilmenite, $FeTiO_3$ (Sec. IV A). A comparison to the Sc^{3+} compounds Sc_2O_3 and ScF_3 is given in Sec. IV B. The

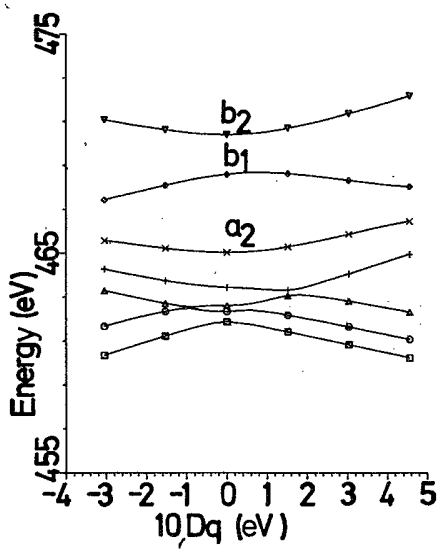

FIG. 6. For Ti^{4+} in O_h symmetry the changes in energy position are given as a function of the crystal-field splitting $10Dq$. The symbols correspond to the seven absorption lines ordered for increasing energy.

scandium compounds show well separated peaks, from which we can show that it is possible to make more accurate comparisons with the exact position of the small leading peaks. Section IV C deals with CaF_2, whose (bulk) spectrum is completely reproduced. We end with a comparison with a series of potassium-halide K $L_{2,3}$ edges,[19] which will be discussed in Sec. IV D.

A. The Ti $L_{2,3}$ XAS spectrum of $FeTiO_3$

We have compared the titanium $L_{2,3}$ edge of $FeTiO_3$ with the calculation of Ti^{4+} in O_h symmetry. The exact structure of $FeTiO_3$ (see Table V) (Refs. 20 and 21) and the resulting point group of Ti^{4+} are not critical for our analysis. Figure 7 gives the $FeTiO_3$ spectrum compared with the calculation in O_h symmetry, which shows good agreement and justifies the approximation of octahedrally surrounded Ti^{4+} ions. Although we will not discuss the theoretical Ti^{3+} spectrum we calculated, we note that the experimental Ti $L_{2,3}$ XAS spectrum of $FeTiO_3$ is only consistent with Ti^{4+}, not Ti^{3+}.[22]

To obtain the optimum agreement with experiment, it is necessary to choose different Lorentzian broadenings for the four peaks. The optimum values for the broadening are given in Table III. After the Lorentzian broadening the whole spectrum was convoluted with a Gaussian broadening of 0.15 eV (Ref. 23) to simulate the experimental resolution. From this choice of broadenings and from the resulting agreement with experiment, *it is clear that each peak in the $L_{2,3}$ XAS spectrum has its own characteristic broadening.* Noticing this we will try to find the underlying reasons. The extra broadening of the peaks belonging to the L_2 edge (peak b_1 and b_2) originates from the shorter lifetime of the $p_{1/2}$ states. A $p_{1/2}$ state has an extra decay channel, the Coster-Kronig (CK) Auger decay process,[5,24] by which it can fall back to a $p_{3/2}$ hole, with the simultaneous ejection of a d electron. The energy difference between a $2p_{1/2}$ and a $2p_{3/2}$ hole, due to the $(2p)$ spin-orbit coupling, must be larger than the binding energy of the d electron, otherwise the CK Auger channel is closed.

From Table III we conclude that the CK Auger broadening of the L_2 edge (peak a_2 and b_2) is 0.4 eV. Subtracting this broadening,[25] both peaks a_2 and b_2 have an extra broadening of about 0.5 eV with respect to peaks a_1 and b_1. The origin of this broadening could be due to (1) a lifetime effect similar to the L_2 CK Auger decay, (2) an effect of the actual point-group symmetry, (3) vibrational (phononic) broadening, and (4) dispersional

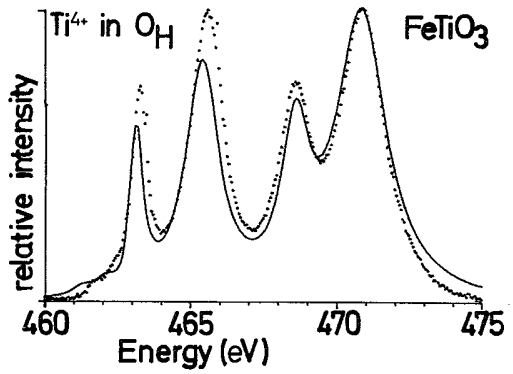

FIG. 7. The experimental $FeTiO_3$ spectrum (dotted), measured with the SX700 monochromator at Berliner Elektronenspeicherring-Gesellschaft für Synchrotronstrahlung m.b.H (BESSY), is compared with a multiplet calculation in O_h symmetry. The crystal-field parameter is 1.8 eV; the broadening factors are tabulated in Table III.

broadening. The possibility of a large broadening effect of a decay process (1) seems unlikely. The energy difference with respect to the lowest main peak is only about 2 eV, which prohibits real Auger decay processes, though virtual processes cannot be excluded. The effect of an actual lower point-group symmetry may be important in the special case of $FeTiO_3$. Because in the other compounds which we will discuss O_h symmetry is better obeyed and their broadenings are equivalent (see Table IV), we do not expect a large extra broadening effect of the reduced symmetry, though in the case of $FeTiO_3$ it may be considerable. In Sec. V we will come back to the possible effect of a lower symmetry and make a connection with the vibrational broadening mechanism. We will now further concentrate on effects (3) and (4), the vibrational and dispersional broadening mechanisms, which can be combined under the heading solid-state broadening.

In a simple picture of a transition metal in octahedral symmetry, the two peaks in both the L_3 and the L_2 edge can be related to t_{2g} (d_{xy}, d_{xz}, and d_{yz} orbitals) and e_g (d_{z2} and d_{x2-y2} orbitals) symmetry.[14] Although in a full atomic multiplet plus crystal-field description this division is not exact, it is a good starting point. In octahedral symmetry e_g orbitals point to the ligands, while t_{2g} orbitals point in between them. This causes the e_g orbitals to bind more strongly to the ligands and conse-

TABLE III. The broadening factors for the $FeTiO_3$ spectrum: The total broadening (Γ) is divided in the Coster-Kronig Auger broadening (α) and the solid-state broadening (β). From the adjustment to experiment it is found that $\alpha=0.4$ eV and $\beta=0.5$ eV (see Fig. 7).

Peak	Total Γ	CK Auger α	Γ-α	Solid state β	Γ-α-β
a_1	0.1 eV		0.1 eV		0.1 eV
a_2	0.6 eV		0.6 eV	0.5 eV	0.1 eV
b_1	0.5 eV	0.4 eV	0.1 eV		0.1 eV
b_2	1.0 eV	0.4 eV	0.6 eV	0.5 eV	0.1 eV

quently to a higher energy of the (antibonding) e_g state, compared to the (antibonding) t_{2g} state. This is in fact the origin of the crystal-field splitting.[14] We can now conclude that, independent of the exact symmetry, the second peak will always be related to a state that has a larger hybridization with the ligands.

Large hybridization, which arises when the states are directed towards the ions, also means that the equilibrium interatomic distances are strongly dependent on occupation of the levels. In x-ray absorption the antibonding levels become occupied, which means that the final-state interatomic distance is larger than the equilibrium ground-state interatomic distance. This is indicated in Fig. 8 [$R^*(e_g) > R\cdot$]. Following the Franck-Condon principle[26] this means a large final-state vibrational broadening (see Fig. 8). For small hybridization (i.e., the t_{2g} orbitals) this Franck-Condon broadening will be smaller. Thus the larger hybridization can cause the extra broadening of the a_2 and b_2 peak. We would also expect a large temperature dependence because of the occupancy of excited vibrational states in the (electronic) ground state. Thermal effects will broaden both the "t_{2g}" and "e_g" states, but the effect on the e_g state will be larger. This thermal broadening more or less scales with the final-state vibrational broadening, which is also present at 0 K [see Fig. 8; compare the energy widths for e_g and t_{2g} at 0 K and at finite temperature (T^*)].

The possibility of dispersional broadening is related to the amount of hybridization. The larger hybridization of the e_g states results in larger bandwidths in the solid state. This dispersion can, however, be reduced or eliminated by excitonic effects due to the large core-hole $3d$ attraction, which localizes the $3d$ electron.[27] The conclusion is that the a_2 and b_2 peaks, because of their larger hybridization, can have stronger vibrational broadening and possibly also stronger dispersional broadening. We do not see a possibility to separate these two broadening mechanisms. Therefore we would like to denote the experimentally found broadening of the e_g peaks in general as a solid-state broadening. This solid-state broadening is found to be 0.5 eV in $FeTiO_3$ (see Table III). From the discussion of the potassium-halide spectra (Sec. IV D), vibrational broadening is found to be the major broadening mechanism.

The analysis procedure of the $FeTiO_3$ $L_{2,3}$ XAS spectrum can be generalized in the following way: First measure the experimental splittings between the a_1 and a_2 peak (ΔL_3) and between the b_1 and b_2 peak (ΔL_2). The splittings found can be related to the value of $10Dq$ with use of the theoretical ΔL versus $10Dq$ lines as given in Fig. 4. With the observed $10Dq$ value, the spectrum can be simulated and from a comparison with the experimental spectrum the exact broadening factors are found.

Although we will not discuss other symmetries in detail, it is interesting to see what happens for a strongly distorted system, such as rutile TiO_2.[28] The strong distortion makes it impossible to simulate its XAS spectrum with the Ti^{4+} p^5d^1 multiplet in O_h symmetry. If the symmetry is reduced to D_{4h}, however, good agreement with experiment can be reached (see Fig. 9).[29] We have used the same range of broadenings as found for $FeTiO_3$. In D_{4h} symmetry the p^5d^1 multiplet consists of 22 lines (seven in O_h). Also one has to consider three crystal-field parameters (only one in O_h) and the polarization dependence of the spectrum. Further discussion of D_{4h} symmetry and the TiO_2 spectrum will be given elsewhere.[18]

B. The Sc $L_{2,3}$ edge of Sc_2O_3 and ScF_3

Figure 10 shows the Sc $L_{2,3}$ edge of Sc_2O_3 overlayed with a calculated spectrum for a crystal field of 1.83 eV. The broadening factors used are given in Table IV. The ScF_3 spectrum, Fig. 11, was measured by Chen *et al.* at Brookhaven National Laboratory (BNL).[19]

The ScF_3 spectrum is similar to Sc_2O_3, but some interesting differences can be seen: The broadening factors for the fluoride are smaller than for the oxide (see Table

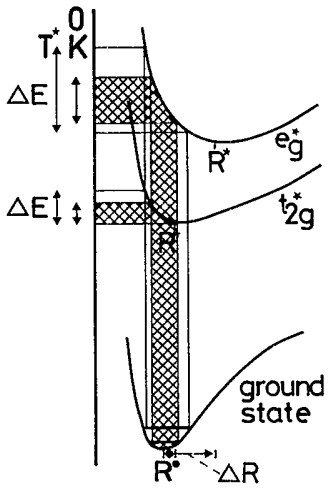

FIG. 8. Because an electron is added to an antibonding e_g or t_{2g} orbital, the equilibrium interatomic distance (R) becomes larger. The largest ΔR occurs for the e_g^* orbital. Following the Franck-Condon principle this leads to the largest broadening (ΔE). Raising the temperature from 0 K (T) to a finite temperature (T^*) enlarges ΔE both for the e_g and t_{2g} peaks.

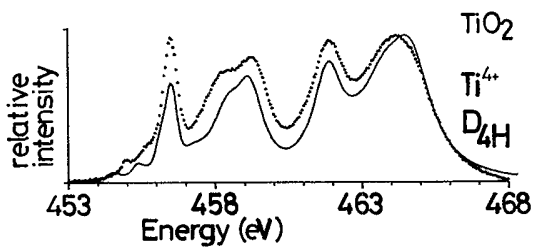

FIG. 9. The experimental TiO_2 spectrum (dotted), measured with the SX700 monochromator at BESSY, is compared with a multiplet calculation in D_{4h} symmetry. The crystal-field parameter ($10Dq$) is 1.8 eV and the values for the 420 and 220 branches are 0.75 and 0.3 eV, respectively; the broadening factors are similar to those for $FeTiO_3$.

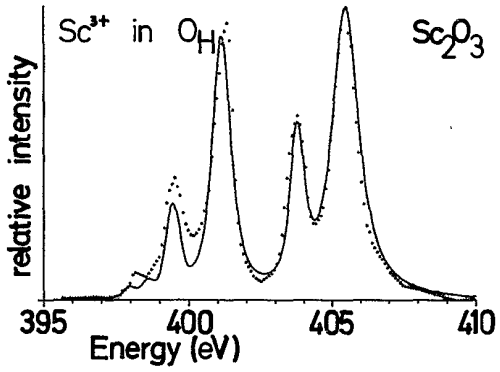

FIG. 10. The experimental Sc_2O_3 spectrum (dotted), measured with the SX700 monochromator at BESSY, is compared with a multiplet calculation in O_h symmetry. The crystal-field parameter is 1.8 eV; the broadening factors are tabulated in Table IV.

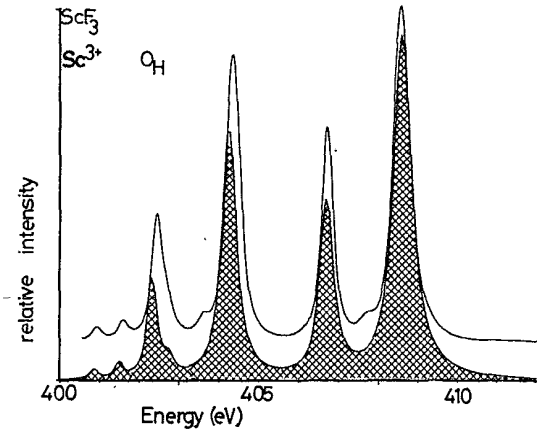

FIG. 11. The experimental ScF_3 spectrum (solid line), measured with the "dragon" monochromator at Brookhaven National Laboratory (BNL) Chen *et al.*, is compared with a multiplet calculation in O_h symmetry (shaded area). The crystal-field parameter is 1.7 eV; the broadening factors are tabulated in Table IV.

IV). Notice that this is no resolution effect, which is taken care of by the extra Gaussian broadening. The small leading peaks come out more clearly in the ScF_3 spectrum: Close comparison of the calculated multiplets with $FeTiO_3$ and Sc_2O_3 (Figs. 7 and 10), shows small discrepancies in the energy position of the leading peaks. In the experimental spectra they are situated closer to the rest of the spectrum. This discrepancy is not found in ScF_3 (and CaF_2, see the next section), which indicates that for the fluorides the Coulomb and exchange parameters (F^2, G^1, and G^3), which dominate the precise energy position of the leading peaks, have the atomic value, and thus are not screened. In our present calculations we used a 20% reduction from the *ab initio* Hartree Fock (HF) values. The reduction to 80% of the HF values originate from the practice of fitting calculated multiplets to atomic data.[15] The reduction results from the inclusion of many-body corrections (configuration interaction) leading to effective parameters.

We can conclude that, while for ScF_3 the atomic approach works out well, the spectra of the oxides indicate that the effective Coulomb and exchange parameters must be further reduced. This leads to leading peaks closer to the rest of the spectrum, but another result is a change in the intensity distribution of the main peaks resulting in a change in the L_3/L_2 branching ratio.[8,9,30,31] The reduction of the intra-atomic interactions in the oxides means that solid-state effects are more important. Covalent screening can cause reduced effective values of the intra-atomic interactions. We find that these screening effects do not play a significant role in ScF_3 and CaF_2 (see Fig. 13), which marks a clear distinction between fluorides and oxides. This agrees with the clearly larger solid-state broadening in the oxides compared with the fluorides (see Table IV) and with the concept that fluorides are more ionic.

C. The Ca $L_{2,3}$ edge of CaF_2

CaF_2 has been frequently studied because of its interesting theoretical and practical aspects.[32–35] With our calculations we are able to disprove the suggestion that the small leading peaks in the $L_{2,3}$ XAS spectrum of

TABLE IV. The broadening parameters for Lorentzian broadening of the individual peaks. σ is the Gaussian broadening factor which simulates the experimental resolution. The individual numbers should not be taken too literally. The trend in the values for the CK Auger (α) and the solid-state broadening (β) is, however, clear. The crystal-field splitting ($10Dq$) shows a trend similar to the broadenings. Notice that all *KX* spectra were fitted with the same broadenings, which were not fully optimized and from which it is not possible to derive values for α and β.

	Peaks							
Compound	a_1	a_2	b_1	b_2	σ	α	β	$10Dq$
KX	0.14	0.22	0.20	0.22	0.03			0.6 (KF) 1.1 (KI)
CaF_2	0.08	0.15	0.10	0.18	0.03	0.02	0.07	−0.9
ScF_3	0.13	0.20	0.19	0.26	0.03	0.06	0.07	1.7
Sc_2O_3	0.10	0.30	0.25	0.45	0.15	0.15	0.20	1.8
$FeTiO_3$	0.10	0.60	0.50	1.00	0.15	0.40	0.50	1.8

CaF_2 are related to Ca^+ ($4s$).[32] Figure 12 shows the spectrum with a crystal-field splitting ($10Dq$) of about -0.9 eV, which compares well with the experimental result for bulk CaF_2 (Ref. 34) [and also for seven layers of CaF_2 on Si (Refs. 32 and 33)]. Notice that negative values of $10Dq$ are used, because the calcium ion is in eightfold coordination (simple-cubic). The two main lines are reproduced, as well as the small leading peaks. In this case the leading peaks also include the low-energy peaks of the crystal-field doublet, the a_1 and b_1 peak, which have low intensity because of the small and negative value of $10Dq$. The ΔL_2 and ΔL_3 splittings deviate strongly from $10Dq$ and from each other, which prohibits a direct explanation of the individual peaks and thus necessitates a full atomic multiplet calculation. Including the crystal field, this can fully explain the Ca $L_{2,3}$ XAS spectrum and the small leading peaks come out "automatically," without recourse to the $4s^1$ configuration.

In Fig. 12 there are some small discrepancies: In the experimental spectrum there exists an extra peak at ~ 352.3 eV (b') and also the a' peak at ~ 348.7 eV is considerably more intense. We believe that this originates from a shifted superposition of the spectrum as a result of surface (or damage) effects. This shift is also observed in a surface study of CaF_2 on Si,[32,33] in which it is suggested that in the surface layer of CaF_2 the Ca ions have an extra $4s$ electron. The (formally) monovalent Ca^+ ions shift the spectrum to lower energy. If this is correct the spectrum originates from a $4s^1$ to $2p^5 3d^1 4s^1$ transition, which can result in a modified multiplet spectrum. To check this we performed a series of calculations with different crystal fields: We calculated the Ca^+ $2p^5 3d^1 4s^1$ in O_h symmetry and also in lower symmetries (D_{4h} and D_{3d}) to make a better simulation of the surface symmetry. Experimentally a polarization dependence is found,[32] which clearly proves the existence of a symmetry lower than O_h. In a future paper we will focus on CaF_2 and discuss the different multiplet calculations in detail.[36]

D. The K $L_{2,3}$ edges of potassium halides

To complete the series of d^0 compounds, we have calculated the potassium $L_{2,3}$ edges from the K^+ $2p^5 3d^1$ multiplets with the crystal-field parameter between 0 and 1 eV, and compared the results with the data of the potassium halides from Sette *et al.*[37]

Our calculations are in excellent agreement with the experimental results. In Fig. 13 the experimental results are compared with approximately the corresponding calculated K^+ $p^5 d^1$ multiplets. We did not optimize our results accurately to the experimental spectra, but the excellent visual agreement makes one sure of the possibility to do so. With the use of the relation between $10Dq$ and the splittings between the main peaks (see Fig. 4), the values for $10Dq$ can be extracted from the experimental spectra. The small inequality of the L_3 and L_2 splittings (Fig. 4) and the small leading peaks are visible in the experiment. The small peaks in between the L_3 and L_2 edge, and the bumps around 300 eV, are not explained by the present multiplet calculation. They are probably related to the $4s$ bands, although there is also a possibility that they originate from a lower symmetry, eventually in combination with surface effects (as for CaF_2).

The four calculated spectra in Fig. 13 are broadened

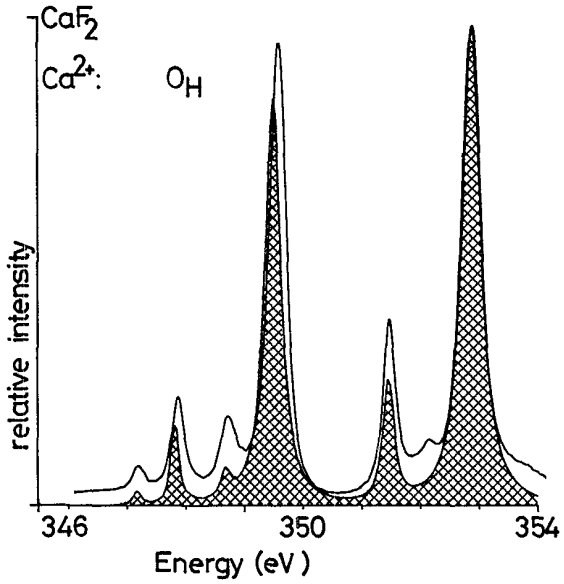

FIG. 12. The experimental CaF_2 spectrum (solid line), measured with the "dragon" monochromator at BNL by Chen *et al.*, is compared with a multiplet calculation in O_h symmetry (shaded area). The crystal-field parameter is -0.9 eV; the broadening factors are tabulated in Table V.

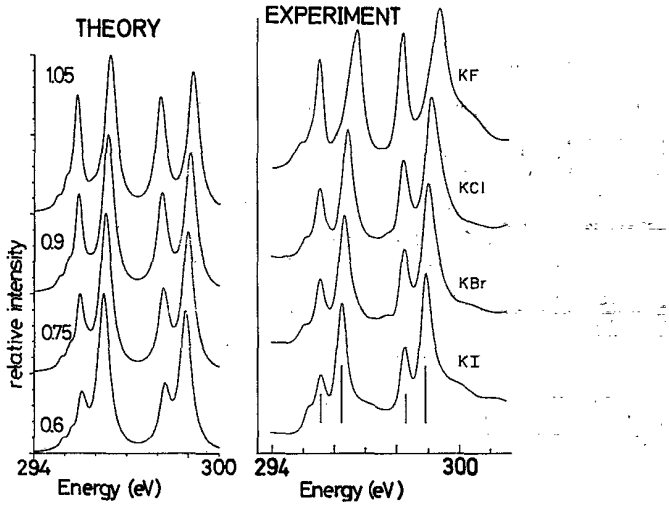

FIG. 13. Four K^+ $2p^5 3d^1$ excitation spectra in O_h symmetry (right side) are compared with the four potassium halide spectra, measured with the dragon monochromator at BNL by Chen *et al.* (left side). The calculated spectra are not completely optimized to the experiment. The broadenings used are adjusted to KI. Notice that the KF spectrum is broader (see text).

with identical broadening factors (see Table IV). Close comparison to the experimental spectra reveals that the a_2 and b_2 peaks are extra broadened for KF compared to KI. Or in other words, the solid-state broadening of the e_g peaks (see Sec. IV B) is considerably larger for KF. Going through the halide series the dominant change is the potassium-halide interatomic distance, as given in Table V. We will examine their relation to the possibility of vibrational and dispersional broadening.

A shorter interatomic distance means that the final-state vibrational broadening will be larger: A shorter distance results in a larger expansion (ΔR) after the filling of the antibonding e_g orbital. KF has shorter interatomic distances than KI, thus KF should have a larger broadening.[38] The trend in the vibrational broadening is thus in agreement with experiment.

Considering the dispersional effects a distinction can be made between broadening due to K^+-halide hybridization and K^+-K^+ hybridization. The direct cation interactions are expected to be smaller and in general they can be neglected for ioniclike compounds. We will, however, shortly consider both possible sources of dispersion. The hybridization with the ligand is expected to be largest for iodide, which would lead to the largest broadening for KI, opposite to the experimental trend. Thus ligand hybridization cannot explain the observed broadenings. Direct cation-cation interactions (K^+-K^+ hybridization) should in rocksalt structure be larger for the t_{2g} orbitals, compared to the e_g orbitals. This is also in contrast with the experimental observation that the a_2 and b_2 peaks (corresponding largely to e_g orbitals) are broader than the a_1 and b_1 peaks (corresponding largely to t_{2g} orbitals).

The conclusion is that both possible sources of dispersional broadening do not agree with the experimental observation. Thus the extra broadening for the e_g peaks in KF is caused by vibrational broadening, which also suggests that, at least for the potassium halides, final-state vibrational broadening is the dominant broadening factor. As can be seen in Table IV the amount of broadening scales with the interatomic distance for all compounds discussed.

TABLE V. The crystal structure and nearest-neighbor metal-ligand distances (R_{ML}) of the discussed compounds. Data from Ref. 28.

Compound	Crystal structure	R_{ML}
KF	rocksalt	2.66
KCl	rocksalt	3.14
KBr	rocksalt	3.29
KI	rocksalt	3.53
CaF_2	fluorite	2.27
ScF_3	cubic ReO_3	2.11*
Sc_2O_3	Re_2O_3-C	2.01*
$FeTiO_3$	ilmenite	1.92(3)
		2.06(3)
TiO_2	rutile	1.94(4)
		1.99(2)

*Reference 27.

V. CONCLUDING REMARKS

We have shown that an atomic multiplet calculation followed by a transformation to a cubic crystal field (O_h symmetry) can reproduce excellently the transition-metal $L_{2,3}$ x-ray-absorption edges of the d^0 compounds discussed. Within this description it becomes clear that the splitting between the two main peaks in both the L_3 and L_2 edge is related, though not equal to the crystal-field splitting $10Dq$. Also the small leading peaks can be explained as a part of the p^5d^1 multiplet. Their position is controlled by the Coulomb and exchange parameters (F^2, G^1, and G^3). The crystal field does not influence them strongly, which causes their uniform appearance in the spectra.

Each main peak has its own individual broadening, which is caused by the Coster-Kronig Auger decay process of the L_2 edge and by the solid-state broadening of the "e_g" peaks. From the discussion of the potassium-halide spectra it becomes clear that the dominant solid-state broadening effect is the final-state vibrational broadening.

The central discriminating factor for the e_g broadening is the interatomic radius. A small radius results in a large broadening and also a large crystal-field splitting. This causes the broadening trend for the potassium halides to be $F^- > Cl^- > Br^- > I^-$, in agreement with the trend in the radii. From this observation it can be concluded that for the potassium halides the crystal-field splitting originates dominantly from ionic factors. The covalent contribution, which can be expected to be largest for iodide, can be neglected in first approximation.

It is shown that the small leading peaks in the fluoride spectra (CaF_2 and ScF_3) fully agree with the "atomic" multiplet spectra. In the oxide spectra, however, the leading peaks are closer to the rest of the spectrum, which is a mark of decreased intra-atomic Coulomb and exchange parameters. In the oxides the effects of the solid state (covalent screening) are so large that the intra-atomic interactions (on the empty $3d$ electron states) are rescaled, while for F^- no effect is found. This marks a different "nature" of the oxides compared to the fluorides. Fluorides can be considered as ionic, while oxides have some important covalent character.

We have shown that with our calculations, which treat the atomic multiplet effects in detail, it becomes possible to separate out the atomic effects from solid-state effects. This makes it possible to study the latter, i.e., the broadening of the peaks, related to the final-state vibrational broadening and the CK Auger decay, the exact position of the small leading peaks, related to the covalent screening of intra-atomic (pd) Coulomb and exchange interactions, and the presence of extra peaks, related to surface effects and/or reduced symmetry.

Finally we point out the relationship between vibrational broadening and the (static) lowering of the symmetry. Vibrations can be viewed as dynamical distortions of the site symmetry. The Franck-Condon principle states that x-ray absorption is a fast process with respect to vibrations. The symmetry of the absorbing (transition-metal) cation is constantly changing. This affects the

XAS spectrum, which in this picture can be viewed as a superposition of all possible distorted site symmetries. The difference with a static symmetry breaking is that in that case a specific point-group symmetry can be applied to all cations, which results in a different spectrum, as for TiO_2. For cases like $FeTiO_3$, with structureless peaks it is not trivial to separate the (small) static lowering of symmetry from the dynamical (vibrational) symmetry-breaking effects. To answer the questions concerning these effects it would be desirable to study a compound more closely, experimentally as well as theoretically. Measurements at low temperatures can reduce the dynamical effects and possibly reveal the static symmetry effects. Theoretically all lower point groups can be calculated, and in principle also the dynamical effects can be simulated.

ACKNOWLEDGMENTS

We are grateful to the staff of the Berliner Elektronenspeicherring-Gesellschaft für Synchrotronstrahlung (BESSY) for their support during the XAS experiments. This work was supported, in part, by the Dutch Foundation for Chemical Research [Stichting Scheikundig Onderzoek Nederland (SON)] with financial assistance of the Netherlands Organization for Scientific Research [Nederlandse Organisatie voor wetenschappelijk Onderzoek (NWO)] and by the Committee for the European Development of Science and Technology (CODEST) program. We also thank C. T. Chen, F. Sette, and F.J. Himpsel for permission to reproduce previously unpublished results.

[1]Examples of high-resolution (1:1000) monochromators in the 300–800-eV range include the SX700 at BESSY, H. Petersen, Nucl. Instrum. Methods A **246**, 260 (1986), and the 10-m grazing-incidence monochromator at Photon Factory, H. Maezawa, S. Nakai, S. Mitani, A. Mikuni, T. Namioka, and T. Sasaki, *ibid.* **246**, 310 (1986).

[2]An even better resolution (up to 1:10 000) is reached by the dragon monochromator at BNL: C. T. Chen, Nucl. Instrum. Methods A **256**, 595 (1987).

[3]Compare the present resolution with, e.g., the resolution reached in 1982 as can be found in R. D. Leapman, L. A. Grunes, and P. L. Fejes, Phys. Rev. B **26**, 614 (1982).

[4]A former description has been given by T. Yamaguchi, S. Shibuya, S. Suga, and S. Shin, J. Phys. C **15**, 2641 (1982).

[5]This approch has been proven very successful for the rare-earth $M_{4,5}$ edges; see, e.g., B. T. Thole, G. van der Laan, J. C. Fuggle, G. A. Sawatzky, R. C. Karnatak, and J. M. Esteva, Phys. Rev. B **32**, 5107 (1985).

[6]For the $L_{2,3}$ x-ray-absorption edges the atomic approach is not sufficient and the crystal field has to be included; see, e.g., B. T. Thole, R. D. Cowan, G. A. Sawatzky, J. Fink, and J. C. Fuggle, Phys. Rev. B **31**, 6856 (1985).

[7]The theoretical basis for this method can be found in R. D. Cowan, J. Opt. Soc. Am. **58**, 808 (1968), and R. D. Cowan, *The Theory of Atomic Structure and Spectra* (University of California Press, Berkeley, 1981).

[8]J. Zaanen, G. A. Sawatzky, J. Fink, W. Speier, and J. C. Fuggle, Phys. Rev. B **32**, 4095 (1985).

[9]J. Fink, Th. Müller-Heinzerling, B. Scheerer, W. Speier, F. U. Hillebrecht, J. C. Fuggle, J. Zaanen, and G. A. Sawatzky, Phys. Rev. B **32**, 4899 (1985).

[10]P. H. Butler, *Point Group Symmetry, Applications, Methods and Tables* (Plenum, New York, 1981).

[11]J. R. Derome and W. T. Sharp, J. Math. Phys. **6**, 1584 (1965).

[12]P. H. Butler and B. G. Wybourne, Int. J. Quantum Chem. **10**, 581 (1976).

[13]E. U. Condon and G. H. Shortley, *The Theory of Atomic Spectra* (Cambridge University Press, Cambridge, 1964).

[14]This part is also nicely discussed by C. J. Ballhausen, in *Introduction to Ligand Field Theory* (McGraw-Hill, New York, 1962).

[15]R. D. Cowan, *The Theory of Atomic Structure and Spectra* (University of California Press, Berkeley, 1981), p. 464, and references therein.

[16]G. van der Laan, B. T. Thole, and G. A. Sawatzky, Phys. Rev. B **37**, 6587 (1988).

[17]F. M. F. de Groot, B. T. Thole, and G. A. Sawatzky (unpublished).

[18]F. M. F. de Groot, B. T. Thole, and G. A. Sawatzky (unpublished).

[19]C. T. Chen and F. Sette (private communication).

[20]A. F. Wells, *Structural Inorganic Chemistry,* 3rd ed. (Clarendon, Oxford, 1962), p. 486.

[21]R. E. Newnham, J. H. Fang, and R. P. Santoro, Acta Crystallogr. **17**, 240 (1963).

[22]J. B. Goodenough, Phys. Rev. **117**, 1442 (1960); Prog. Solid State Chem. **5**, 145 (1972).

[23]With a Gaussian broadening of 0.15 eV we mean that the parameter σ is chosen as 0.15 eV; this also applies for the Lorentzian broadenings.

[24]J. Zaanen and G. A. Sawatzky, Phys. Rev. B **33**, 8074 (1986).

[25]This procedure is not exact, but it is good enough for the accuracy needed.

[26]C.-O. Almbladh and L. Hedin, in *Handbook on Synchrotron Radiation,* edited by E. E. Koch (North-Holland, Amsterdam, 1983), Vol. 1, p. 635.

[27]D. K. G. de Boer, C. Haas, and G. A. Sawatzky, Phys. Rev. B **29**, 4401 (1984).

[28]A. F. Wells, Ref. 20, p. 461.

[29]Our spectrum is equivalent to the EELS spectrum of Brydson *et al.*, R. Brydson, B. G. Williams, W. Engel, H. Sauer, E. Zeitler, and J. M. Thomas, Solid State Commun. **64**, 609 (1987).

[30]B. T. Thole and G. van der Laan, Phys. Rev. B **38**, 3158 (1988).

[31]G. van der Laan and B. T. Thole, Phys. Rev. Lett. **60**, 1977 (1988).

[32]D. Rieger, F. J. Himpsel, U. O. Karlsson, F. R. McFreely, J. F. Morar, and J. A. Yarmoff, Phys. Rev. B **34**, 7295 (1986).

[33]F. J. Himpsel, U. O. Karlsson, J. F. Morar, D. Rieger, and J. A. Yarmoff, Phys. Rev. Lett. **56**, 1497 (1986).

[34]C. T. Chen and F. Sette, Phys. Rev. Lett. **60**, 160 (1988).

[35]F. J. Himpsel, U. O. Karlsson, J. F. Morar, D. Rieger, J. A. Yarmoff, Phys. Rev. Lett. **60**, 161 (1988).

[36]F. J. Himpsel *et al.* (unpublished).

[37]F. Sette, B. Sinkovic, Y. J. Ma, and C. T. Chen, Phys. Rev. B **39**, 11 125 (1989).